# Noise-induced effects on period-doubling bifurcation for integrate-and-fire oscillators

Takashi Tateno*
*Graduate School of Engineering Science, Osaka University, 1-3 Machikaneyama, Toyonaka-shi, Osaka 560-8531, Japan*
(Received 31 August 2000; revised manuscript received 16 July 2001; published 9 January 2002)

This study provides a method for calculating first-order approximations of the Lyapunov exponents of systems with discontinuity in the presence of noise in order to characterize the stability of motions in those systems. This paper in particular illustrates the results of the ways in which noise influences period-doubling bifurcation in the parameter space of an integrate-and-fire model with a periodically modulated reset level. For evaluating a stochastic version of period-doubling bifurcation, the first-passage-time problem of the Ornstein-Uhlenbeck process is used to define a Markov operator governing the transition of a reset-level phase density. The results on the stochastic bifurcation are thus compared with numerical computations of angles and moduli of eigenvalues of the Markov operator that describes the firing properties of the model.

DOI: 10.1103/PhysRevE.65.021901 PACS number(s): 87.15.Aa, 87.15.Ya, 87.17.Nn

## I. INTRODUCTION

Nonlinear systems perturbed by noise have the potential to display a wide range of nontrivial and complex phenomena. This range includes the enhancement of order in the system as well as the destabilization of the system's behavior [1]. The theoretical and numerical study of random dynamical systems has been receiving a lot of attention in recent years [2], and notable examples of noise-induced phenomena that have been investigated include stochastic resonance [3], noise-induced order [4], and noise-induced chaos [5,6].

Noise-induced chaos was first observed in the behavior of a driven nonlinear oscillator [5] and was later studied using the noisy logistic map [4,6]. The main finding of these studies was that intrinsic noise truncates the period-doubling cascade to chaos. That is, the periodic motions with high periods of the noise-free systems are replaced by chaoslike motions when noise is added. Period-doubling bifurcation in the pure sense will not always appear in physical systems because the presence of noise will alter the original bifurcation. Since the period-doubling route to chaos is characteristic of nonlinear dynamical systems, we have asked how is it that the complete period-doubling cascade is suppressed or masked by noise?

Oseledec has proposed that the attractors of finite-dimensional nonlinear dynamical systems can be characterized by values called Lyapunov characteristic numbers, or Lyapunov exponents [7]. Calculating the Lyapunov exponents of ''smooth'' dynamical systems is a well-developed subject on which a lot of literature is available [8], but in many fields we also need to consider ''nonsmooth'' dynamical systems with discontinuities. For example, an algorithm for ''smooth'' dynamical systems is not directly applicable to machine dynamics that are due to impulses or to integrate-and-fire oscillations that are due to a threshold process.

Müller has presented a model-based algorithm for calculating the Lyapunov exponents of dynamical ''nonsmooth'' systems with discontinuities [9]. In the present work we extend that method to noisy systems and use the method to characterize the stability of nonsmooth dynamical systems in the presence of additive noise. We are thus able to present a method for obtaining a first-order approximation of the Lyapunov exponents of such systems.

This paper focuses on the simplest and most widely studied model of biological oscillators, the integrate-and-fire (IF) oscillator [10]. This model captures some of the spiking properties of a neuron and was constructed according to a phenomenological approach with the intention of matching the basic behavior displayed by the biologically realistic Hodgkin-Huxley model [11,12]. Whenever the state of the IF oscillator crosses some threshold, the oscillator fires and there is then a discontinuity as it resets. Although the discontinuous nature of the changes makes a complete description in terms of ''smooth'' differential equations impossible, it is possible to apply dynamical approaches to classify the bifurcation of IF models with a periodic reset level as tangent (saddle-node) and period-doubling bifurcations [13].

In this paper we describe noise-induced effects on the bifurcation of an IF model in which the reset level is periodically modulated and, in particular, we describe the effects obtained in the parameter regions in which period-doubling bifurcation occurs. We start by presenting a method for calculating the Lyapunov exponents of the model and use the method to evaluate the effects of noise on the stability of the system. We then use the spectra of a Markov operator to analyze the stochastic bifurcation in the system. Finally, the results on stochastic bifurcations are compared with numerical computations of angles and moduli of the eigenvalues of the Markov operator that describes the firing properties of the model.

## II. THE LYAPUNOV EXPONENTS OF NOISY INTEGRATE-AND-FIRE OSCILLATORS

Consider a noisy one-dimensional nonlinear dynamical system with discontinuities in the neighborhood of the action of a discontinuity, in particular, the system called an IF oscillator. The noisy IF model is described by a stochastic differential equation

*FAX: +81-66843-9354.
Email address: tateno@bpe.es.osaka-u.ac.jp

 

$$dX(t)=f(X(t),t)dt+\sigma dW_t, \tag{1}$$

$$X(0)=x_0, \tag{2}$$

where $f(x,t)$ is a function in $C^1$ for $x$ and $t$, the constant $\sigma$ is a noise intensity, and $W_t$ denotes the standard Wiener process. Furthermore, the variable $X(t)$ must be subject to a resetting mechanism, and this is described by

$$X(t_n^-)\equiv\lim_{\varepsilon\to 0}X(t_n-\varepsilon)=h(t_n),$$
$$X(t_n^+)\equiv\lim_{\varepsilon\to 0}X(t_n+\varepsilon)=g(t_n), \tag{3}$$

where $h(t)$ and $g(t)$ are smooth functions in $C^1$. In neural models, the functions

$$f(x,t)=F(x)+I(t) \tag{4}$$

and

$$F(x)=-\frac{x}{\tau}, \tag{5}$$

where $\tau$ is a time constant and $I(t)$ represents an input term, are often used. The properties of the model are characterized by sequences of firing times, where the firing times are defined as

$$T_k=\inf\{t|X(t)\geqslant h(t);t\geqslant T_{k-1}>t_0;X(0)=x_0\}. \tag{6}$$

The system can thus be expressed by the following set of equations:

$$X(0)=x_0, \tag{7}$$

$$dX(t)=f(X(t),t)dt+\sigma dW_t,\quad (t_{k-1}<t<t_k)\quad (k=1,2,\ldots) \tag{8}$$

$$X(t_k^-)=h(t_k)\quad (k=1,2,\ldots), \tag{9}$$

$$X(t_k^+)=g(t_k)\quad (k=1,2,\ldots). \tag{10}$$

Müller, using an idea for the study of impact oscillators, has proposed a method for calculating the Lyapunov exponents of a discontinuous dynamical system [9]. Müller introduced a perturbed dynamics $\tilde{X}(t)$ and directly calculated the deviation between perturbed and unperturbed trajectories. First, suppose that an initial deviation $\Delta x_0$ between the perturbed and unperturbed trajectories is positive and denote the subsequent deviations as $\Delta X(t)$. We then have

$$\tilde{X}(0)=x_0-\Delta x_0, \tag{11}$$

$$\tilde{X}(t)=X(t)-\Delta X(t). \tag{12}$$

The firing times of the perturbed system are defined as

$$\tilde{T}_k=\inf\{t|\tilde{X}(t)\geqslant h(t);t\geqslant\tilde{T}_{k-1}>t_0;\tilde{X}(0)=x_0-\Delta x_0\}, \tag{13}$$

and the behavior of the perturbed system is governed by the following set of equations:

$$\tilde{X}(0)=x_0-\Delta x_0, \tag{14}$$

$$d\tilde{X}(t)=f(\tilde{X}(t),t)dt+\sigma dW_t,\quad (\tilde{t}_{k-1}<t<\tilde{t}_k)\quad (k=1,2,\ldots), \tag{15}$$

$$X(\tilde{t}_k^-)=h(\tilde{t}_k)\quad (k=1,2,\ldots), \tag{16}$$

$$X(\tilde{t}_k^+)=g(\tilde{t}_k)\quad (k=1,2,\ldots). \tag{17}$$

If the firing times satisfy the relations $t_1\leqslant\tilde{t}_1\leqslant t_2$ and $\tilde{t}_1<(t_1+t_2)/2$, for instance, one obtains, for the perturbed motion, a first discontinuity at the time

$$\tilde{t}_1=t_1+\Delta t_1. \tag{18}$$

Similarly, for two series $\{t_k\}$ and $\{\tilde{t}_k\}$ $(k=1,2,\ldots)$, we can define a time difference $\Delta t_k$

$$\Delta t_k=\tilde{t}_{l(k)}-t_k, \tag{19}$$

where $\tilde{t}_{l(k)}$ is the nearest-neighboring firing time of $t_k$ in the perturbed firing sequence.

If $\Delta t$ is sufficiently small, we can apply a stochastic Taylor expansion to approximate $X(t+\Delta t)$ in the vicinity of any given $t$ with an expression in the first order of $\Delta t$,

$$X(t+\Delta t)\approx X(t)+f(X(t),t)\Delta t+\sigma\Delta W_t, \tag{20}$$

where $\Delta W_t$ is the increment of the Wiener process

$$\Delta W_t=W_{t+\Delta t}-W_t. \tag{21}$$

From Eqs. (12), (16), (19), and (20) we have

$$
\begin{aligned}
0 &= \tilde{X}(\tilde{t}^{-}_{l(k)}) - h(\tilde{t}_{l(k)}) = \tilde{X}(t_k^- + \Delta t_k) - h(t_k + \Delta t_k) \\
&\approx \tilde{X}(t_k^-) + f(\tilde{X}(t_k^-), t_k^-)\Delta t_k + \sigma \Delta W_{t_k} - h(t_k) - h'(t_k)\Delta t_k \\
&\approx X(t_k^-) - \Delta X(t_k^-) + f(X(t_k^-), t_k^-)\Delta t_k + \sigma \Delta W_{t_k} - h(t_k) \\
&\quad - h'(t_k)\Delta t_k \\
&= -\Delta X(t_k^-) + \sigma \Delta W_{t_k} + [f(X(t_k^-), t_k^-) - h'(t_k)]\Delta t_k . \qquad (22)
\end{aligned}
$$

The time difference

$$
\Delta t_k = \frac{\Delta X(t_k^-) - \sigma \Delta W_{t_k}}{f(X(t_k^-), t_k^-) - h'(t_k)} \qquad (23)
$$

is thus obtained. In the same way, from Eqs. (12), (17), (19), and (20) we obtain

$$
\begin{aligned}
\Delta X(\tilde{t}^{+}_{l(k)}) &= X(t_k^+ + \Delta t_k) - \tilde{X}(t_k^+ + \Delta t_k) \\
&= X(t_k^+ + \Delta t_k) - g(t_k + \Delta t_k) \\
&\approx X(t_k^+) + f(X(t_k^+), t_k^+)\Delta t_k \\
&\quad + \sigma \Delta W_{t_k} - g(t_k) - g'(t_k)\Delta t_k \\
&= [f(X(t_k^+), t_k^+) - g'(t_k)]\Delta t_k + \sigma \Delta W_{t_k} . \qquad (24)
\end{aligned}
$$

From Eqs. (23) and (24) we obtain

$$
\Delta X(\tilde{t}^{+}_{l(k)}) = \frac{f(X(t_k^+), t_k^+) - g'(t_k)}{f(X(t_k^+), t_k^+) - h'(t_k)} \Delta X(t_k^-) + \sigma \frac{f(X(t_k^-), t_k^-) - f(X(t_k^+), t_k^+) + g'(t_k) - h'(t_k)}{f(X(t_k^-), t_k^-) - h'(t_k)} \Delta W_{t_k} . \qquad (25)
$$

For convenience, we can write this in the form

$$
\Delta X(\tilde{t}^{+}_{l(k)}) = a_k \Delta X(t_k^-) + \sigma(1 - a_k)\Delta W_{t_k}, \qquad (26)
$$

where

$$
a_k = \frac{f(X(t_k^+), t_k^+) - g'(t_k)}{f(X(t_k^-), t_k^-) - h'(t_k)} . \qquad (27)
$$

Suppose, for example, that the $k$th firing of the unperturbed system occurred at a time $t$ between the firing times $\tilde{t}_{l(k)}$ and $\tilde{t}_{l(k-1)}$ of the perturbed system. Then $X(t)$ of Eq. (1) is expressed by

$$
X(t) = X(\tilde{t}^{+}_{l(k-1)}) + \int_{\tilde{t}^{+}_{l(k-1)}}^{t} f(X(s), s) ds + \sigma \int_{\tilde{t}^{+}_{l(k-1)}}^{t} dW_s , \qquad (28)
$$

where $\int_{\tilde{t}_{l(k-1)}}^{t} dW_s$ represents the Ito integral. From this equation we know that, for $t \leqslant \tilde{t}_{l(k)}$,

$$
\Delta X(t) = \Delta X(\tilde{t}^{+}_{l(k-1)}) + \int_{\tilde{t}^{+}_{l(k-1)}}^{t} [f(X(s), s) - f(\tilde{X}(s), s)] ds . \qquad (29)
$$

For the function specified in Eq. (5), this equation may be simplified to

$$
\Delta X(t) = \exp[-(t - \tilde{t}^{+}_{l(k-1)})/\tau]\Delta X(\tilde{t}^{+}_{l(k-1)}) . \qquad (30)
$$

From Eqs. (26) and (30) we have

$$
\begin{aligned}
\Delta X(t_k^-) = \exp[-(t_k - t_{k-1})/\tau] \{ & a_{k-1} \Delta X(t_{k-1}^-) \\
& + \sigma(1 - a_{k-1}) \Delta W_{t_{k-1}} \} . \qquad (31)
\end{aligned}
$$

We so far assumed that the deviation $\Delta x_0$ between the initial values of the perturbed and unperturbed systems is positive, but Eq. (31) also holds in the case of a negative deviation. By applying Eq. (31) recursively, we obtain

$$
\begin{aligned}
\Delta X(t_k^-) = {} & a_{k-1} \cdots a_2 a_1 \exp[-(t_k - t_1)/\tau] \Delta X(t_1^-) + \sigma a_{k-1} \cdots a_2 (1 - a_1) \exp[-(t_k - t_1)/\tau] \Delta W_{t_1} \\
& + \sigma a_{k-1} \cdots a_3 (1 - a_2) \exp[-(t_k - t_2)/\tau] \Delta W_{t_2} \\
& \vdots \\
& + \sigma a_{k-1} (1 - a_{k-2}) \exp[-(t_k - t_{k-2})/\tau] \Delta W_{t_{k-2}} + \sigma (1 - a_{k-1}) \exp[-(t_k - t_{k-1})/\tau] \Delta W_{t_{k-1}} \\
= {} & \left( \prod_{j=1}^{k-1} a_j \right) \exp[-(t_k - t_0)/\tau] \left[ \Delta X_0 + \sigma \sum_{j=1}^{k-1} \left( \prod_{i=1}^{j} a_i^{-1} \right) (1 - a_j) e^{(t_j - t_0)/\tau} \Delta W_{t_j} \right] . \qquad (32)
\end{aligned}
$$

For a large integer $n$, we can define

$$\lambda_n(\sigma,x_0,\Delta x_0)=\frac{1}{(t_n-t_0)}\ln\left|\frac{\Delta X(t_n)}{\Delta X_0}\right|$$
$$=\frac{1}{(t_n-t_0)}\ln\left|\left(\prod_{j=1}^{n-1}a_j\right)\exp[-(t_n-t_0)/\tau]\left[1+\sigma\sum_{j=1}^{n-1}\left(\prod_{i=1}^{j}a_i^{-1}\right)(1-a_j)e^{(t_j-t_0)/\tau}\Delta W_{t_j}/\Delta X_0\right]\right|$$
$$=-\frac{1}{\tau}+\frac{1}{(t_n-t_0)}\ln\left|\left(\prod_{j=1}^{n-1}a_j\right)\left[1+\sigma\Delta x_0^{-1}\sum_{j=1}^{n-1}\left(\prod_{i=1}^{j}a_i^{-1}\right)(1-a_j)e^{(t_j-t_0)/\tau}\Delta W_{t_j}\right]\right|. \quad (33)$$

Hence we can calculate a stochastic version of the Lyapunov exponent $\lambda(\sigma,x_0)$ proposed by Müller if there exists

$$\lambda(\sigma,x_0)=\lim_{\Delta x_0\to 0}\lambda(\sigma,x_0,\Delta x_0)$$
$$=\lim_{\Delta x_0\to 0}\{\lim_{n\to\infty}\lambda_n(\sigma,x_0,\Delta x_0)\}. \quad (34)$$

There are cases where the mapping represented by $l(k)$ in Eq. (19) is not one-to-one and, in such cases, the mapping is not invertible. That is, for example, more spikes may appear along one trajectory than along the corresponding perturbed trajectory. Generally, in cases where two or more spikes occur along the unperturbed trajectory between $\tilde{t}_k$ and $\tilde{t}_{k+1}$, this calculation might underestimate the Lyapunov exponent because the effects of noise on the unperturbed system have not been fully included in the process of estimation. However, since, in the numerical simulation, the two series $\{t_k\}$ and $\{\tilde{t}_{k'}\}$ coincide, except for a few of the earliest firing times, actually calculating the value remains meaningful. In the following section, the result of the numerical calculation will be discussed in terms of this topic.

## III. A NOISY INTEGRATE-AND-FIRE MODEL WITH A PERIODIC RESET LEVEL

In the absence of noise, the periodic modulation of the reset level in IF models can still lead to rich dynamics. IF models with periodic modulation of the reset level (or threshold) are meant to mimic cells with external periodic forcing, or with internal periodic forcing such as arises in certain types of bursting (e.g., slow wave bursting) [14]. Such modulation of IF models is able to produce period-doubling and saddle-node bifurcations. The period-doubling routes to chaos in IF models have been numerically demonstrated and have been confirmed by directly evaluating the Lyapunov exponents of the models [13,15]. In this section we take a particular interest in those IF models that include periodic modulation of the reset level and we show how it is possible to numerically approximate the Lyapunov exponents in the presence of noise.

Consider a constant external input $[I(t)=I_0]$, a time-invariant threshold $[h(t)=1]$, and a sinusoidally modulated reset level $g(t)$. That is, $g(t)=A\sin\{2\pi(t+\theta_0)\}$, where $2\pi\theta_0$ ($\theta_0\in[0,1]$) is an initial phase of the periodic modulation. Note that, to allow the use of dimensionless parameters and variables in the equation for $g(t)$, the period of the reset level has been normalized to 1 and the mean amplitude has been set to zero. Hence the parameter $\tau$ is the ratio of the frequency of the periodically modulated reset level to the firing frequency of the noiseless ($\sigma=0$) oscillator governed by Eq. (1). From Eq. (27) we obtain

$$a_k=\frac{\tau I_0-A\sqrt{1+(2\pi\tau)^2}\sin\{2\pi(t_k+\theta_0)+\alpha\}}{\tau I_0-1}, \quad (35)$$

where

$$\alpha=\arctan(2\pi\tau). \quad (36)$$

In the absence of noise, as Coombes has reported [15], the Lyapunov exponents of the systems are independent of any initial value or of any initial deviation, and the deterministic $\lambda_n$ is described by

$$\lambda_n=-\frac{1}{\tau}+\frac{1}{(t_n-t_0)}\sum_{j=1}^{n}\ln|a_j|. \quad (37)$$

The output of the model consists of a sequence of firing times. Figure 1(a) shows (deterministic) bifurcation diagrams that depict the dependence of interspike intervals on the amplitude $A$ of modulation of the reset level.

There is no fixed phase relation in the quasiperiodic range ($0<A<0.28$), so the dots are scattered throughout the intervals. The fixed phase relations in the 1:1 mode-locked range ($0.28<A<0.546$) are presented as a single dot for each $A$ value. With increasing $A$, the first period-doubling bifurcation from period 1 to 2 and the second bifurcation from period 2 to 4 occur near $A=0.546$ and $A=0.640$, respectively. The corresponding dependence of the Lyapunov exponent is shown in Fig. 1(b). Since for a large $n$ (e.g., $n=5000$), the ratio of $\lambda_n$ to $\lambda_{n+1}$ is approximately equal to 1 (i.e., $|\lambda_{n+1}/\lambda_n-1|<10^{-6}$), we can regard $\lambda_n$ as the Lyapunov exponent. The Lyapunov exponent rises above zero near $A=0.68$ and tends to increase with higher values of $A$. This implies that the motion in the model is a chaoslike oscillation.

A forward Euler algorithm with a fixed step size of 0.001 time units was used in numerically calculating the noisy model. However, in a numerical calculation, we are unable to obtain idealized white noise. In order to investigate the noise correlation, the autocorrelation function of the noise we used

was calculated. This showed that our simulated noise provided a good approximation of white noise.

After simulating the tracks of the two trajectories when the initial deviation $\Delta x_0$ was small, we used Eq. (33) to calculate the $\lambda_n(\sigma,x_0,\Delta x_0)$ with $n=10\,000$. The numerical calculation showed that, in a mode-locked region of parameter space, even with a low noise level (e.g., $\sigma=0.0001$), the two trajectories eventually coincided within a finite number of steps (e.g., within less than $n=50$). The two series $\{t_k\}$ and $\{\tilde{t}_{k'}\}$ thus coincide with the exception of a few of the firing times early in the numerical simulation, so that the number of spikes along the unperturbed trajectory which do not form pairs with spikes along the perturbed trajectory is limited. Thus, in the mode-locked region of the numerical simulation, spikes from two series always form such pairs. In the quasiperiodic and chaotic parameter regions, in contrast,

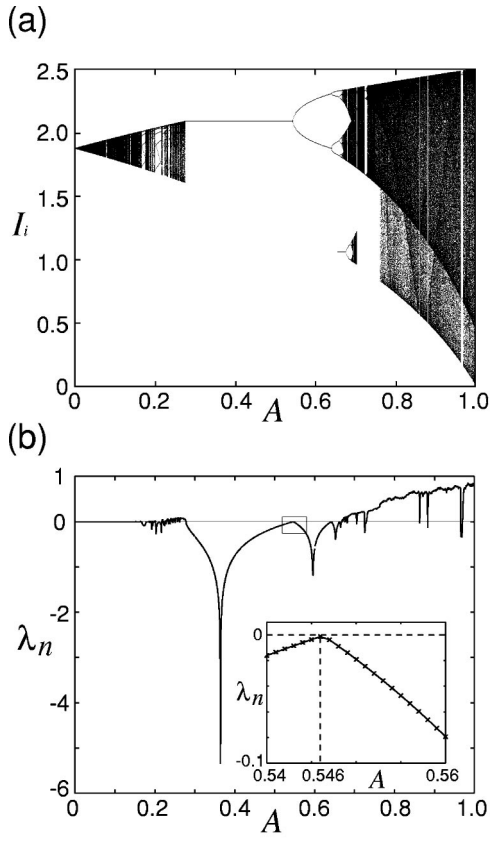


FIG. 1. (a) A deterministic bifurcation diagram of Eq. (1) with a periodic reset level $g(t)=A\sin\{2\pi(t+\theta_0)\}$ and a constant threshold $h(t)=1$ in the absence of noise ($\sigma=0$). This IF model shows the dependence of quasiperiodic, phase-locked, and chaoslike oscillations on the amplitude $A$ of modulation of the reset level. The plot is of the interspike-interval sequence $\{I_{1000},\ldots,I_{1100}\}$, where $I_i=T_{i+1}-T_i$ ($i=1000,\ldots,1100$), versus $A$. Other parameters: $\tau=1$ and $I(t)\equiv I_0=1.2$. (b) A plot of the Lyapunov exponent versus the amplitude $A$ in the absence of noise ($\sigma=0$). Parameter values of the IF model are the same as those used to obtain part (a). The inset is an expanded view of the plot over the interval [0.54, 0.56]. Around $A=0.546$ and $A=0.640$ the Lyapunov exponents are approximately equal to zero and this corresponds to the period-doubling bifurcations from period 1 to period 2 and from period 2 to period 4, respectively. Other parameters: $\tau=1$ and $I_0=1.2$.

a small amount of noise did not always result in a coincidence between the two trajectories.

Thus, to calculate the exponential terms in Eq. (33) under the limitations of the possible numerical ranges of computers, we must, in practice, select intermediate noise intensities the trajectories coincide and the terms vanish after the coincidence. In the numerical calculations, we included counting the number of spikes that do not form pairs with one member in the unperturbed trajectory and one in the perturbed trajectory. For example, for the range of quasiperiodic behavior (e.g., $A=0.27$) the average numbers of nonmatching spikes resulting from 1000 realizations of the Wiener process were $0.244\pm0.437$ (mean $\pm$ standard deviation) and zero when $\sigma=0.05$ and $\sigma=0.001$, respectively. The corresponding numbers for the parameter range (e.g., $A=0.75$) that produces chaotic behavior were $0.64\pm0.553$ and $2.05\pm1.46$ when $\sigma=0.05$ and $\sigma=0.001$, respectively. One order reversal of appearance of the respective elements of the pairs in the two firing time-series $\{t_k\}$ and $\{\tilde{t}_{k'}\}$ creates no problem for this calculation because we are still able to find the spike of one series corresponding to that of the other. However, when two or more reversals of order in the firing times of the two series occur, it may not be possible to find some spikes along one trajectory which correspond to spikes along the other trajectory. In such cases, the Lyapunov exponents are underestimated by this numerical calculation, as was stated in the preceding section.

We selected various initial deviations ($\Delta x_0$) from 0.0001 to 0.01 and various initial values ($x_0$) from the interval [0,1] and calculated the resulting values of $\lambda_n(\sigma,x_0,\Delta x_0)$. With these deviations and initial conditions, the numerical calculation brought no significant difference of the values of $\lambda_n$, so that the results remained unchanged. The average of $\lambda_n(\sigma,x_0,\Delta x_0)$ ($\sigma=0.005$, 0.01, 0.02, and 0.03) calculated for 1000-times realization of the Wiener process is plotted against $A$ in Fig. 2(a), where the error bars show the standard deviation. Overall, for larger noise intensities (e.g., $\sigma\geqslant0.03$) the Lyapunov exponents are larger in the presence of noise than in the absence of noise. In general, the stability of a system can be characterized by the largest Lyapunov exponent. One can thus see that noise decreases the stability of the IF model in the sense that the (negative) Lyapunov exponent increases and crosses zero as the noise intensity increases.

However, at intermediate noise levels, the dependence of the Lyapunov exponent on the noise intensities is markedly affected by the way the oscillator behaves. Figure 2(b) shows plots of the average of the Lyapunov exponents (ALEs) as a function of noise intensity and shows different noise-intensity dependences for the three typical behaviors of the IF model: oscillations that are chaoslike ($A=0.75$), mode locked ($A=0.47$), and quasiperiodic ($A=0.25$). When noise is added to the deterministic IF model while it is in the region of the chaoslike oscillation, the ALE falls gradually as the noise intensity increases. As the noise intensity increases, while the model is in the region of mode-locked oscillation, however, the ALE first decreases and then increases. This means that increasing the noise intensity beyond a certain

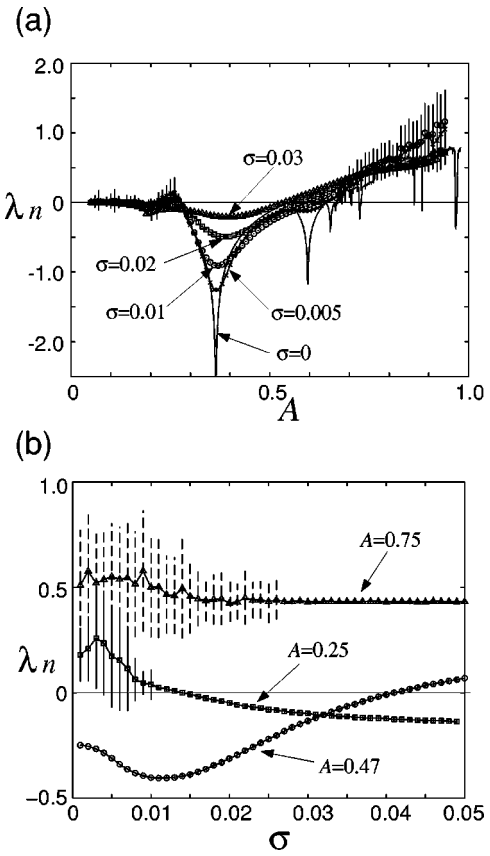


FIG. 2. (a) Lyapunov exponent $\lambda_n$ versus amplitude $A$ for $n=10\,000$ in the presence of noise. The curves show averages for 1000-times realization of the standard Wiener process, and error bars show the standard deviation. $\sigma=0$, 0.005, 0.01, 0.02, and 0.03. These plots correspond to the deterministic plot given in Fig. 1(b). Other parameters: $\tau=1$, $I_0=1.2$, $\Delta x_0=0.001$, and $x_0=0$. (b) Lyapunov exponent $\lambda_n$ versus the noise intensity $\sigma$ for $n=10\,000$. The curves show averages for 1000-times realization of the standard Wiener process, and the error bars show the standard deviation. A=0.25 (squares), 0.47 (circles), and 0.75 (triangles). In the case of $A=0.47$, the standard deviations of $\lambda_n$ are so small that we are unable to see the error bars clearly in the scale, but the size of the vertical lines are given in the labels of the circles in the plot. Other parameters: $\tau=1$, $I_0=1.2$, $\Delta x_0=0.001$, and $x_0=0$.

value leads to ''destabilization'' of the system. As the noise intensity increases, while the model is in the region of quasiperiodic oscillation, the ALE first increases to a maximum value and then falls. This means that increasing noise intensity leads to ''stabilization'' of the system. The plot also shows that, in chaoslike and quasiperiodic oscillations, the fluctuations in $\lambda_n$ are larger at small noise intensities ($\sigma<0.01$) than at larger noise intensities.

## IV. SPECTRAL ANALYSIS OF A MARKOV OPERATOR

In the preceding section, the index (Lyapunov exponent) as numerically calculated from the series of firing times has been dealt with in order to determine the property of stability of the IF model. However, from the direct numerical calculation, we can only have realizations of such series. In this section, another approach is used. That is, since the firing times are random variables, we can use a stochastic approach to characterize the sequence of firing times.

When $X(0)=g(0)$, the time $T_{\theta_0}$ at which $X(t)$ reaches the threshold $h$ for the first time is called the first-passage time

$$T_{\theta_0}=\inf\{t|X(t)\geqslant h(t);X(0)=g(0)\}. \tag{38}$$

The time $T_{\theta_0}$ has a probability density function (PDF) $G(h(t),t|\theta_0)$ which satisfies the following equation [16]:

$$p(x,t|g(0),0)=\int_0^t G(h(u),u|\theta_0)p(x,t|h(u),u)du,$$
$$[x\geqslant h(t),h(t)>g(t)], \tag{39}$$

where $p(x,t|y,s)$ is the transition PDF of the unrestricted process $X(t)$ and satisfies the following Fokker-Planck equation [16]:

$$\frac{\partial p}{\partial t}=-\frac{\partial}{\partial x}\left[\left\{-\frac{x}{\tau}+I\right\}p\right]+\frac{1}{2}\sigma^2\frac{\partial^2 p}{\partial x^2}. \tag{40}$$

Since the initial phase $\theta_0$ completely determines the time course of the reset level in a PDF of the form $G(h(t),t|\theta_0)$, if we use $G(t|\theta_0)$ to denote the PDF and define

$$f(\theta|\theta_0)=\sum_{n=0}^{\infty} G(n+\theta-\theta_0|\theta_0), \tag{41}$$

then the convergence of the right-hand side of Eq. (41) is ensured [17]. The function $f(\theta|\theta_0)$ satisfies $\int_0^1 f(\theta|\theta_0)d\theta=1$ and $f(\theta|\theta_0)\geqslant 0$ (i.e., the PDF) and is the PDF of the next firing phase given a previous firing phase of $\theta_0$. Let $h_n(\theta)(0\leqslant\theta<1)$ be the PDF of the reset-level phase at the time of the $n$th firing ($n=1,2,\ldots$). Then, $h_n(\theta)$ can be expressed by the following equation:

$$h_n(\theta)=\int_0^1 f(\theta|\theta_0)h_{n-1}(\theta_0)d\theta_0$$
$$\equiv\mathcal{P}h_{n-1}(\theta)(n=1,2,\ldots), \tag{42}$$

where $h_0$ is the PDF of the initial phase $\theta_0$. That is, it satisfies $\int_0^1 h_0(\theta_0)d\theta_0=1$ and $h_0(\theta_0)\geqslant 0$. The operator $\mathcal{P}$ is a Markov operator with the kernel $f(\theta|\theta_0)$. We can inductively obtain $h_n$ by iteratively applying the operator $\mathcal{P}$ to the PDF $h_0$, and $\{\mathcal{P}h_0\}$ is asymptotically stable [18,19]. There thus exists a unique invariant density $h^*$ such that $\mathcal{P}h^*=h^*$ [20]. The PDF of the interspike interval between the $n$th and $(n+1)$th spikes, denoted by $i_n$, is given by

$$i_n(t)=\int_0^1 G(t|\theta)h_{n-1}(\theta)d\theta \quad (n=1,2,\ldots) \tag{43}$$

and the invariant interspike-interval PDF $i^*(t)$ then satisfies

$$i^*(t) = \int_0^1 G(t|\theta) h^*(\theta) d\theta. \tag{44}$$

Since the evolutionary properties of the sequence $\{h_n\}$ defined by Eq. (42) are governed by the operator $\mathcal{P}$, the kernel $f(\theta|\theta_0)$ has all the information needed to describe the evolution of the system's dynamical behavior. The operator $\mathcal{P}$ is linear and its eigenvalues and the corresponding eigenfunctions play a prominent role in determining the behaviors of the sequence $\{h_n\}$. Here, as usual, the eigenvalues are defined as the set of complex numbers $\lambda$ for which there exists a nontrivial $h$ such that $\mathcal{P}h = \lambda h$. Moreover, in general, a spectrum of the operator $\mathcal{P}$ is defined as the set of complex numbers $\lambda$ such that $\mathcal{P} - \lambda I$ is not invertible, where $I$ is the identity operator. However, $\mathcal{P}$ is an infinite-dimensional operator, so that it is possible for its spectrum to be an infinite set that, strictly, contains infinitely many eigenvalues. Nevertheless, the eigenvalues of $\mathcal{P}$ satisfy $|\lambda| \leqslant 1$, while $\lambda = 1$ is itself an eigenvalue. Furthermore, when $\inf_\theta f(\theta|\theta_0) > 0, |\lambda| < 1$ for all eigenvalues that are not one. To analyze the spectral properties of the kernel, we used a numerical calculation of the first-passage time of the Ornstein-Uhlenbeck process $X(t)$ rather than numerically solving the stochastic differential equation of Eq. (1) [21]. This approach enabled us to evaluate the precise structure of the kernel within the limits on the accuracy of the numerical calculation.

Even though the operator $\mathcal{P}$ is of infinite dimension, approximate values for some of the eigenvalues of an operator similar to $\mathcal{P}$ were estimated by replacing $\mathcal{P}$ with a finite-dimensional square matrix that we obtained by discretizing the phases $\theta_0$ and $\theta$. In numerical calculation, the kernel corresponds to the stochastic (transition probability) matrix denoted by a real $M \times M$ square matrix $A_M$. To investigate the characteristics of the kernel, we applied spectral analysis to the stochastic matrix [18]. Another numerical method for calculating the spectrum of an operator similar to $\mathcal{P}$ has been proposed (for those readers who are interested in this subject, see Ref. [22]), but the stochastic matrix is used here. Since $A_M$ is a stochastic matrix and is irreducible, the first eigenvalue of the matrix also satisfies $\lambda_1 = 1$ [23] and there is an eigenfunction (a characteristic vector) that has positive coordinates and corresponds to $\lambda_1$ [19].

Suppose that the eigenvalues $\{\lambda_i\}$ $(i = 1,2, \ldots,)$ of $\mathcal{P}$ are sorted in descending order according to their moduli. If $\lambda_i$ $(i \geqslant 2)$ is complex, we can use the imaginary unit $j$ and denote the eigenvalues as $\lambda_i = r_i \exp(j 2\pi\omega_i)$. Let $e_i(\theta)$ be the corresponding eigenfunction of $\lambda_i$. Then, applying the operator $\mathcal{P}$ to the eigenfunction $e_i$ $k$ times, we have

$$\mathcal{P}^k e_i = \lambda_i^k e_i = r_i^k \exp(j 2\pi k \omega_i) e_i \quad (k = 1,2, \ldots). \tag{45}$$

Note that the first eigenfunction $e_1$ is in accordance with an invariant density $h^*$ and $\lambda_1 = 1$.

Figure 3 shows the invariant interspike-interval density $[i^*(t)]$ diagram obtained from Eq. (44) for a noise intensity $(\sigma = 0.005)$ corresponding to the deterministic bifurcation diagram plotted in Fig. 1(a). The invariant density $(h^*(\theta))$ was calculated by finding the characteristic vector that corresponds to the eigenvalue $\lambda_1 = 1$ from the stochastic matrix $A_M$ of size $M = 100$. From Eq. (45), we can see that the speed at which the sequence $\{h_n\}$ converges to its invariant density is determined by the eigenvalues other than the first $(\lambda_1 = 1)$. In practice, 2000 iterations [i.e., applying the operator to any initial phase density $h_0(\theta)$ 2000 times] seemed to be enough to numerically obtain a function that was approximately equal to the invariant density $h^*$ or $e_1$. Since several of the subsequent eigenvalues, i.e., those other than the first $(\lambda_2, \ldots, \lambda_5)$, play an important role, we need to pay particular attention to the lower-order eigenvalues.

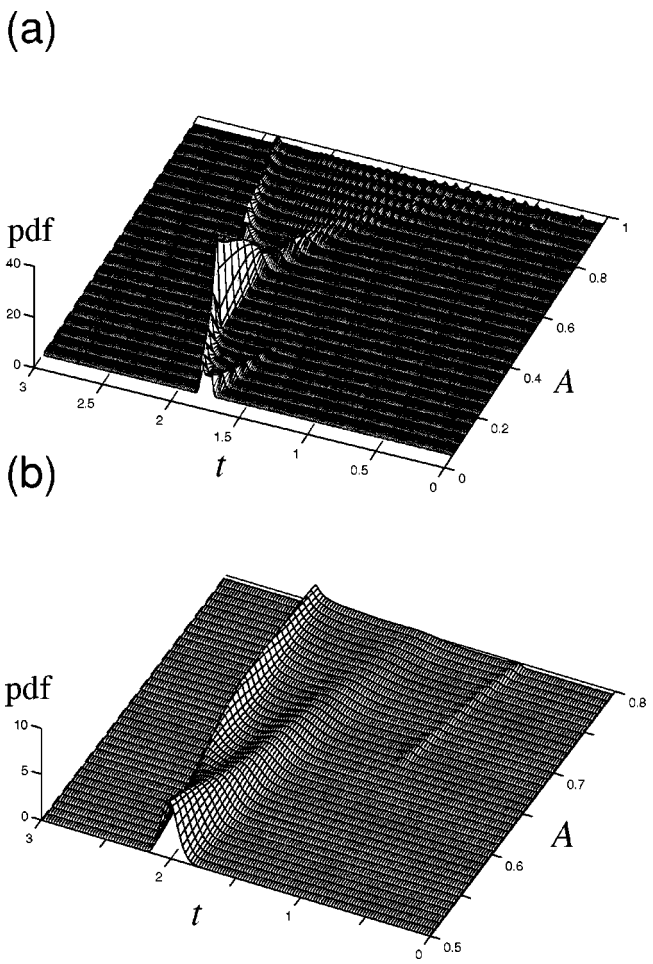


FIG. 3. (a) Invariant interspike-interval density $[i^*(t)]$ diagram for a noise intensity $\sigma = 0.005$. The invariant (phase) density $[h^*(\theta)]$ was first calculated by finding the characteristic vector that corresponds to the eigenvalue $\lambda_1 = 1$ from the stochastic matrix $A_M$ of size $M = 100$. Then, the interspike-interval density was calculated from Eq. (44). This diagram corresponds to the deterministic bifurcation diagram shown in Fig. 1(a) in that $\tau = 1$ and $I_0 = 1.2$. Interspike-interval densities are plotted versus $A$ for each of 90 $A$ values that are equally spaced on the interval [0.05, 0.95]. (b) Expanded view of the diagram in the region where $A$ ranges from 0.5 to 0.8.

Figure 4 shows moduli $(r_2, \ldots, r_5)$ and angles $(2\pi\omega_2, \ldots, 2\pi\omega_5)$ of the second to fifth eigenvalues $(\lambda_2, \ldots, \lambda_5)$ plotted against the amplitude $A$ of the reset level for a fixed noise intensity $(\sigma = 0.002)$. Near $k = 0.52$ [marked $B_1$ in Fig. 4(b)] angles of the second eigenvalue

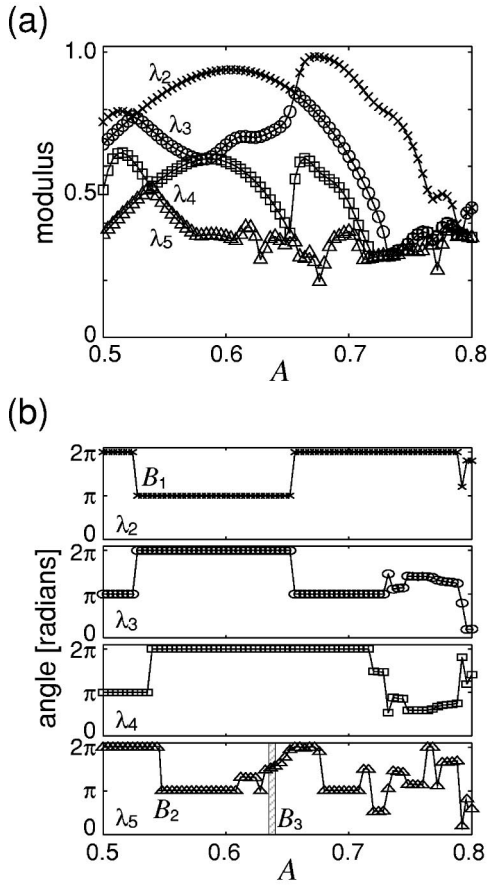


FIG. 4. (a) Moduli of the second to fifth eigenvalues ($\lambda_2, \ldots, \lambda_5$) of the kernel $f(\theta|\theta_0)$ versus the amplitude $A$ of the reset level. (b) Angles of the second and fifth eigenvalues versus the amplitude $A$. Matrix size $M=100$. Other parameters: $\sigma=0.002$, $\tau=1$, and $I_0=1.2$.

change from $2\pi$ to $\pi$ rad. That is, $\lambda_2=r_2\exp(j\pi)$ and the relation

$$\mathcal{P}^2 e_2=\lambda_2^2 e_2=r_2^2\exp(j2\pi)e_2=r_2^2 e_2 \tag{46}$$

holds. Near that point, angles of the third, fourth, and fifth eigenvalues also change from $\pi$ to $2\pi$ rad, but the change in the angle of the fifth eigenvalue seems similar to that of the second. This implies that the first period-doubling bifurcation (period 1 to period 2) occurs in a stochastic sense. For the range beyond that point, each invariant interspike-interval density function has the similar two-peak topological structure which is shown in Fig. 3(b). In the absence of noise, moreover, we are able to observe the second period-doubling bifurcation near $A=0.640$ (cf. Fig. 1). Whereas we are unable to see a change in the angles of the second to fourth eigenvalues with increasing $A$ in the range $0.57<A<0.67$, the angle of the fifth eigenvalue only shows changes for values beyond $A=0.615$. Thus, when $A$ increases, the property related to period four first emerges in the parameter range $0.645<A<0.665$ [the narrow hatched range marked $B_3$ in Fig. 4(b)]. In that range, angles of the fifth eigenvalue are $3\pi/2$ rad. That is, $e_5=r_5\exp(j3\pi/2)$. So the relation

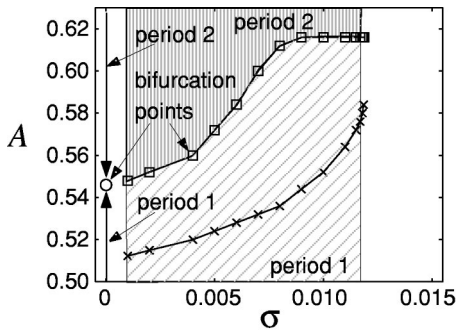


FIG. 5. Point at which the first period-doubling bifurcation from period 1 to period 2 takes place ($\sigma=0$, circle) and the corresponding stochastic bifurcation points (squares), versus noise intensities, in the $\sigma$-$A$ plane. The points at which angles of the second eigenvalue change from $2\pi$ to $\pi$ rad (referred to as points $B_1$, $\times$) are also plotted. Other parameters: $\tau=1$ and $I_0=1.2$.

$$\mathcal{P}^4 e_5=\lambda_5^4 e_5=r_5^4\exp(j6\pi)e_5=r_5^4 e_5 \tag{47}$$

holds. This implies that the second period-doubling bifurcation (period 2 to period 4) occurs in a stochastic sense. Instead of using the second eigenvalue as the definition of the stochastic period-doubling bifurcation [18,19], it is natural to use the fifth eigenvalue to define the stochastic bifurcation. Here, we refer to the point at which angles of the fifth eigenvalue change from $2\pi$ to $\pi$ rad as the stochastic period-doubling bifurcation point that marks the change from period 1 to period 2.

The deterministic first period-doubling bifurcation point (i.e., the first point of bifurcation in the absence of noise) and dependence of the corresponding stochastic period-doubling points on noise intensity is shown in Fig. 5. In the figure, the points at which angles of the second eigenvalue change from $2\pi$ to $\pi$ rad are also plotted and referred to as points $B_1$ in the remainder of this description. The stochastic bifurcation point and point $B_1$ monotonically increase as the noise intensity increases and both suddenly disappear at around $\sigma=0.012$. Over that value ($\sigma=0.012$) there are no changes from $2\pi$ to $\pi$ rad of angles of the second and the fifth eigenvalues. Instead, the angle remains $2\pi$ rad [cf., Fig. 4(b)]. In the definition here, therefore, the stochastic bifurcation point within a small range above zero of noise intensity [i.e., $\lim_{\sigma\to 0}\lambda(\sigma,x_0,\Delta x_0)$] seems to be in accord with the deterministic bifurcation point. Figure 5 shows, however, that if we use the second eigenvalue to define the stochastic period doubling, the alternative bifurcation point (i.e., point $B_1$) with a small range above zero of the noise intensity is not in accord with the deterministic bifurcation point.

## V. DISCUSSION

This paper has concentrated on the interplay between deterministic and stochastic properties of the IF oscillator in those parameter regions where mode-locking, quasiperiodic,

and chaoslike oscillations are observed. We started by showing that, at intermediate levels of noise, the dependence of the Lyapunov exponents on noise intensities is markedly affected by the way the oscillator behaves. Thus, the effects of noise on the stability of the model depend on both the noise intensity and the type of oscillation.

We then paid special attention to the effects of noise on the period-doubling route to chaos. When a period-doubling cascade occurs in a chemical reaction [24] or a biological system [25], only the first few period-doubling bifurcations are observable because the fine structure of the later bifurcations can be masked by noise. Since period-doubling bifurcations are characteristic of nonlinear dynamical systems and the noise effects reported on here are therefore observed in a wide range of other nonlinear systems, our results provide a quantitative measure of the effect of noise on nonlinear systems.

The study of ''qualitative changes'' in parametrized families of random dynamical systems is in general called ''stochastic bifurcation theory'' [2], and recent studies of random dynamical systems have shed light on a dynamical aspect of stochastic bifurcation. In this context, the largest Lyapunov exponent in the presence of noise is used as an index that characterizes the stochastic bifurcation on the basis of the existence of multiple invariant measures. However, in the IF model reported on here, there is only one invariant measure, so that there is no bifurcation in the sense in which the term is used in Ref. [2].

Another definition of stochastic bifurcation is based on the topological structure of invariant densities, and such bifurcation is referred to as phenomenological bifurcation. As shown in Fig. 3(b), when the noise intensity is low, the topological structure of the plot of the invariant interspike-interval density function on the interval-$A$ plane gradually changes with increasing $A$: the plot changes from that of a function with one peak to that of the one with two peaks. In this phenomenological bifurcation, however, we are unable to find an abrupt change as that seen in a deterministic tangent and period-doubling bifurcations [cf. Fig. 1(a)]. In contrast, the definition in the present study allows us to find a clear change of characteristics in this model by using the Markov operator that governs the transition of a reset-level phase density to evaluate a stochastic version of the bifurcations.

There might be no discrepancy between the stochastic period-doubling bifurcation point within a small range above zero of noise intensity and the corresponding bifurcation point in the absence of noise (cf. Fig. 5) when we use the fifth eigenvalues of the stochastic matrix in this definition. However, if we use the second eigenvalues to define the stochastic bifurcation points, we have a discrepancy between the stochastic bifurcation point and the corresponding deterministic bifurcation point. For example, the results of the noisy IF model show that, with an intermediate noise intensity (e.g., $\sigma=0.01$ in Fig. 5), the first period-doubling bifurcation points (i.e., the $B_1$ points), as defined by using the second eigenvalues, coincides with the corresponding bifurcation point of the noiseless IF model. As we have already reported in the previous paper [26], this discrepancy does not arise in the tangent (saddle-node) bifurcations of the noisy IF models. That is, even though the stochastic bifurcation is defined by using the second eigenvalues, the tangent bifurcation point of the noisy IF model approaches the corresponding tangent bifurcation point of the noiseless IF model when the noise intensity is sufficiently low.

Inoue *et al*. have already pointed out a similar problem and shown the difference between the stochastic tangent and period-doubling bifurcation points that appears when a method that uses the spectra of a Markov operator is applied to a noisy sine-circle map [27]. They report that, if the stochastic period-doubling bifurcation point from period 1 to 2 is defined as the point at which the angle of the second eigenvalue changes from 0 to $\pi$ rad, the definition does not work well within a small range above zero of noise intensity. Instead, they define the value of the bifurcation parameter at which the third eigenvalue takes it maximum as the period-doubling bifurcation point from period 1 to period 2. While the definition of the stochastic period-doubling bifurcation point presented in this paper differs from their definition, their results show that the higher-order eigenvalues also have information that explains the stochastic period-doubling bifurcation. The method presented in this paper has thus been to analyze the eigenvalues and eigenfunctions of the Markov operator of the IF model. The first eigenfunction, which corresponds to the first eigenvalue $\lambda_1=1$, has static information such as an invariant density. In contrast, the results of this work show that the higher-order eigenvalues and eigenfunctions have dynamic information that characterizes the stochastic bifurcation defined here.

## ACKNOWLEDGMENTS

This work was in part supported by a Grant-in-Aid for Scientific Research (B)(2)12480086 from the Japan Society for the Promotion of Science. I thank Professor C. E. Smith (North Carolina State University) and Professor S. Sato (Osaka University) for valuable discussions.

[1] F. Moss and P.V.E. McClintock, *Noise in Nonlinear Dynamical Systems* (Cambridge University Press, Cambridge, 1987), Vols. 1–3.

[2] L. Arnold, *Random Dynamical Systems* (Springer-Verlag, Berlin, 1998).

[3] J.K. Douglass *et al.*, Nature (London) **365**, 337 (1993); K. Weisenfeld and F. Moss, *ibid.* **373**, 33 (1995); J.J. Collins, C.C. Chow, and T.T. Imhoff, *ibid.* **376**, 236 (1995); J.J. Collins *et al.*, J. Neurophysiol. **76**, 642 (1996).

[4] K. Matsumoto and I. Tsuda, J. Stat. Phys. **31**, 87 (1983).

[5] J.P. Crutchfield and B.A. Huberman, Phys. Lett. A **77**, 407 (1980).

[6] J.P. Crutchfield, J.D. Farmer, and B.A. Huberman, Phys. Rep. **92**, 46 (1982).

[7] V.I. Oseledec, Trans. Mosc. Math. Soc. **19**, 197 (1968).
[8] *Lyapunov Exponents*, edited by L. Arnold, H. Crauel, and J.-P. Eckmann (Springer-Verlag, Berlin, 1990).
[9] P.C. Müller, Chaos Solitons Fractals **5**, 1671 (1995).
[10] B.W. Knight, J. Gen. Physiol. **59**, 734 (1972); S. Kauffman, Bull. Math. Biol. **36**, 171 (1974); J.P. Keener, J. Math. Biol. **12**, 215 (1981).
[11] A.L. Hodgkin and A.F. Huxley, J. Physiol. (London) **117**, 500 (1952).
[12] L.W. Abbott and T.B. Kepler, in *Statistical Mechanics of Neural Networks*, edited by L. Garrido, Lecture Notes in Physics Vol. 368 (Springer-Verlag, Berlin, 1990), pp. 5–18.
[13] L. Glass and M.C. Mackey, J. Math. Biol. **7**, 339 (1979); J.P. Keener, F.C. Hoppensteadt, and J. Rinzel, SIAM (Soc. Ind. Appl. Math) J. Appl. Math. **41**, 503 (1981).
[14] X.-J. Wang and J. Rinzel, in *Handbook of Brain Theory and Neural Networks*, edited by M.A. Arbib (MIT Press, Cambridge, 1995), p. 689.
[15] S. Coombes, Phys. Lett. A **255**, 49 (1999).
[16] L.M. Ricciardi and S. Sato, in *Lectures in Applied Mathematics and Informatics*, edited by L.M. Ricciardi (Manchester University Press, New York, 1990).
[17] S. Sato, J. Appl. Probab. **14**, 850 (1977).
[18] S. Doi, J. Inoue, and S. Kumagai, J. Stat. Phys. **90**, 1107 (1998).
[19] T. Tateno *et al.*, J. Stat. Phys. **78**, 917 (1995); **92**, 675 (1998).
[20] A. Lasota and M.C. Mackey, *Chaos, Fractals, and Noise: Stochastic Aspects of Dynamics*, 2nd ed. (Springer-Verlag, New York, 1994).
[21] A. Buonocore, A.G. Nobile, and L.M. Ricciardi, Adv. Appl. Probab. **19**, 784 (1987).
[22] T. Shimokawa *et al.*, Biol. Cybern. **83**, 327 (2000).
[23] F.R. Gantmacher, *The Theory of Matrices* (Chelsea Publishing Company, New York, 1959), Vol. II.
[24] G. Rabai, J. Phys. Chem. A **101**, 7085 (1997).
[25] G.A. Ruiz, Chaos Solitons Fractals **6**, 487 (1995).
[26] T. Tateno and Y. Jimbo, Phys. Lett. A **271**, 227 (2000).
[27] J. Inoue, S. Doi, and S. Kumagai, in Proceeding of NOLTA '97 Hilton Hawaiian Village, Hawaii, 1997 (unpublished); pp. 13–16; Proceedings of NOLTA '98, Le Regent, Crans-Montana, Switzerland, 1998 (unpublished), pp. 871–874.